PROTEINS: Structure, Function, and Genetics 22:45–54 (1995)

The Essential Dynamics of Thermolysin: Confirmation of the Hinge-Bending Motion and Comparison of Simulations in Vacuum and Water

D.M.F. van Aalten,[1] A. Amadei,[1] A.B.M. Linssen,[1] V.G.H. Eijsink,[2] G. Vriend,[3] and H.J.C. Berendsen[1]
[1]Department of Biophysical Chemistry, University of Groningen, 9747 AG Groningen, The Netherlands;
[2]Laboratory of Microbial Gene Technology, NLH, IBF, Agricultural University of Norway, 1432 Ås, Norway; and
[3]Biocomputing, EMBL, 69117 Heidelberg, Germany

ABSTRACT **Comparisons of the crystal structures of thermolysin and the thermolysin-like protease produced by *B. cereus* have recently led to the hypothesis that neutral proteases undergo a hinge-bending motion. We have investigated this hypothesis by analyzing molecular dynamics simulations of thermolysin in vacuum and water, using the essential dynamics method. This method is able to extract large concerted atomic motions of biological importance from a molecular dynamics trajectory. The analysis of the thermolysin trajectories indeed revealed a large rigid body hinge-bending motion of the N-terminal and C-terminal domains, similar to the motion hypothesized from the crystal structure comparisons. In addition, it appeared that the essential dynamics properties derived from the vacuum simulation were similar to those derived from the solvent simulation.**

Key words: neutral protease, mobility, molecular dynamics

INTRODUCTION

Thermolysin (TLN) is a thermostable member of a group of homologous *Bacillus* metalloendopeptidases or "neutral proteases" (NPs).[1] Crystal structures are available for TLN[2,3] and for the NP produced by *B. cereus* (NP-cer).[4,5] NPs contain 300–319 residues, divided in an N-terminal (mainly β-sheet) and a C-terminal (mainly α-helical) domain, connected by a central α-helix (residues 134–157 in TLN numbering).[2–5] The active site, containing a catalytically essential zinc, is located in a cleft between the N- and C-terminal domains, on the connecting α-helix.

Comparison of the TLN and NP-cer crystal structures led to the hypothesis that NPs exhibit a hinge-bending motion, with residues near position 134 acting as hinge residues.[5,6] This hinge-bending motion supposedly opens and closes the NP active site by a concerted rigid body motion of the N-terminal and C-terminal domains. The hinge-bending hypothesis was further supported by the analysis of the structures of thermolysin and a thermolabile mutant at the end of a molecular dynamics (MD) simulation.[7] Comparison of these structures showed a hinge-bending displacement similar to that observed in the comparison of the thermolysin and NP-cer crystal structures.[5,6] Unfortunately, comparing static structures can lead only to the conclusion that there is a hinge-bending *displacement*. The existence of a hinge-bending *motion*, that is, opening and closing of the active site, can be proven only by methods which analyze protein dynamics. To analyze possible hinge-bending motions, we have performed the essential dynamics analysis[8] on two simulations of TLN. The essential dynamics method is able to extract large concerted atomic motions from an MD trajectory, as has, for example, been demonstrated for lysozyme.[8] Here, we present the results of the application of the essential dynamics method to a TLN solvent simulation. Subsequently, we have performed the same analysis of a TLN vacuum simulation. The comparison of the essential dynamics properties of both simulations appeared to be a useful method to investigate whether the simulations in solvent and vacuum have common essential motions.

MATERIALS AND METHODS

The TLN solvent MD run with periodic boundary conditions has been described elsewhere.[7] In short, this run was performed with the GROMOS program suite[9] and was based on the thermolysin crystal structure.[2,3] All functional ions (four calciums and one zinc) and crystal water molecules were included. The protein was placed in a box filled with water molecules from a liquid configuration.[10] This system (27,646 atoms) was equilibrated for 35 ps, followed by a 90 ps data generation run. In addition, a TLN

Received October 4, 1994; revision accepted January 19, 1995.

Address reprint requests to H.J.C. Berendsen, Department of Biophysical Chemistry, University of Groningen, Nijenborgh 4, 9747 AG Groningen, The Netherlands.
Present address of D.M.F. van Aalten: Department of Biochemistry and Molecular Biology, University of Leeds, Leeds LS2 9JT, U.K.

vacuum run was performed with identical parameters (including crystallographic water molecules). However, periodic boundary conditions and pressure coupling were not applied and the GROMOS reduced charges force field[9] was used. The lengths of the equilibration period and data generation run were chosen the same as for the solvent simulation for the purpose of comparison.

The essential dynamics method (described elsewhere by Amadei et al.[8]) allows identification of the essential degrees of freedom in a protein from an MD trajectory. These essential degrees of freedom are large concerted atomic motions. First, all translational motion in a protein MD trajectory is removed by translation of the center of mass in each frame. Rotational motion is then removed by a least-squares fitting procedure. Subsequently, a covariance matrix is constructed from the resulting trajectory. Here we have used a C_α trajectory to construct the covariance matrix. C_α atoms have been shown to contain all information for a reasonable description of the protein large concerted motions.[8] The covariance matrix is defined by

$$M_{ij} = \langle (x_i - x_{i,0})\,(x_j - x_{j,0}) \rangle$$

in which $x_{i/j}$ are the separate x,y,z coordinates of the C_α atoms and x_0 are the average coordinates. The average is taken over the whole trajectory. Upon diagonalization of the covariance matrix, a set of eigenvectors/eigenvalues is obtained. These eigenvectors represent a direction in a multidimensional space (dimension $3N$, where N is the number of C_α atoms) along which a concerted motion of atoms takes place. The amplitude of each motion is indicated by the corresponding eigenvalue. Construction of a plot of eigenvector indices against eigenvalues, where the eigenvectors are sorted by decreasing eigenvalue (see Fig. 1), shows that there are only a few eigenvectors with large eigenvalues. Analysis of the motions along the other eigenvectors shows simple Gaussian fluctuations. The central hypothesis of the essential dynamics method is that only the motions along the eigenvectors with large eigenvalues are important for describing the functionally significant motions in the protein. These eigenvectors span a plane in the multidimensional space in which most of the motion takes place. The motions along eigenvectors with small eigenvalues are small Gaussian fluctuations orthogonal to this plane. The motion along any desired eigenvector can be inspected by projecting all frames from the MD trajectory on the eigenvector. A new trajectory is generated which, upon visual inspection, reveals large concerted motions of atoms. In contrast to normal mode analysis,[11,12] the essential dynamics method does not assume harmonicity of the motion and can be applied to a subset of coordinates (e.g., only C_α atoms).

There are several essential dynamics properties which can be compared for two trajectories. The dimension of the essential spaces can be compared by calculating the positional distributions for the motions along all eigenvectors and comparing them with ideal Gaussian distributions derived from the amplitude (eigenvalue) of the eigenvector motions. This comparison yields a correlation coefficient, which can be plotted as a function of the eigenvector number. If the spaces in which the motions take place are to be similar for the two simulations, similar plots should be obtained, indicating similar sizes of the essential spaces.

The essential dynamics analysis can be performed on a combined trajectory (constructed by concatenating the trajectories). This method is a powerful tool to evaluate similarities and differences between the essential motions in different trajectories of the same protein. If the motions are similar, then the eigenvalues (and eigenvectors) coming from the separate trajectories and the combined trajectory should be similar. The curves of the correlation coefficients between the positional distributions calculated from the eigenvector motions and ideal Gaussians (described above) should also be similar, indicating similar dimensions of the three essential spaces (that of the two single trajectories and of the combined trajectory). By projecting the two single trajectories on the eigenvector set calculated from the combined trajectory, information can be obtained about differences in fluctuations and equilibrium structures along eigenvectors calculated from the combined trajectory. If the average projections of the two separate trajectories on a specific eigenvector from the eigenvector set calculated from the combined trajectory are different, then this indicates that the equilibrium structures along that direction are different (static shift). Large differences in the positional fluctuations around the average positions of these projections indicate that in the trajectory with the small positional fluctuations, the direction defined by the eigenvector (from the combined trajectory) is a near constraints (nonessential) direction, while for the other trajectory, the same direction belongs to the essential space (change in dynamic properties). However, for most eigenvectors, these changes will not be large enough to enable a clear distinction between an essential and a near constraints direction.

It is known from the comparison of the TLN and NP-cer crystal structures that the root mean squares deviation (RMSD) on the C_α's after superposition of the two N-terminal domains is small.[5,6] The same is true for the superposition of the C-terminal domains. However, if the two complete structures are superposed, the RMSD becomes significantly higher, which indicates that there is a difference in the hinge-bending angle. This principle can be used to determine the position of the hinge.

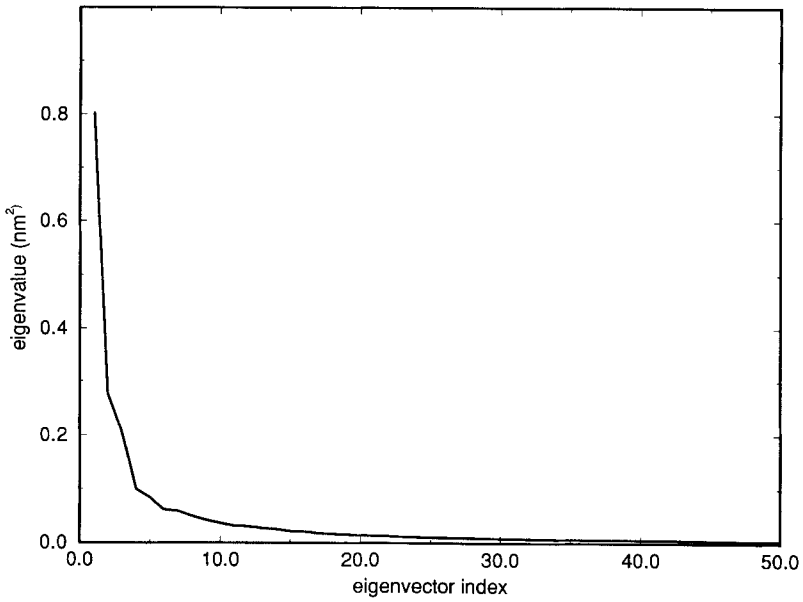

Fig. 1. Plot of eigenvalues against corresponding eigenvector indices derived from the covariance matrix constructed from the solvent simulation. The eigenvectors are sorted by decreasing eigenvalues.

- Structure "A" is superposed on structure "B," which differs in hinge bending angle using only the first part of the N-terminal domain for the fit.
- For each residue I, the C_α–C_α distance from residue I in structure "A" to residue I in structure "B" is calculated.
- These distances are then sorted in a plot according to increasing I–X distance, where X is residues at the edge of one of the domains (here we use Thr-26 for TLN and NP-Cer).

Ideally, the first part of this plot should show a flat line fluctuating near zero (because the fit in the N-terminal domain is good). When it reaches the hinge, the slope should start increasing, indicating that the distances between the residue I pairs become increasingly larger as I moves further away from Thr-26. Such a plot allows us to roughly estimate the position of the hinge. The same procedure can be repeated with superposition on the last part of the C-terminal domains. A similar plot is obtained, but with short distances between the residue pairs in the C-terminal domain. The point where the two plots intersect should be the hinge-bending residue. The results of the application of this method on TLN and NP-cer are shown in Figure 5.

All structure manipulations and inspection of the (eigenvector) trajectories were performed with WHAT IF.[13]

RESULTS AND DISCUSSION

Analysis of the Hinge-Bending Motions

Figure 1 shows a plot of the eigenvector index against eigenvalues, both derived from the covariance matrix constructed from the solvent simulation trajectory. There are only a few eigenvectors with large eigenvalues, which is similar to eigenvector/eigenvalue sets obtained for lysozyme,[8] HPr,[14] and haloalkane dehalogenase (Linssen et al., unpublished results).

The components of the first four eigenvectors are shown in Figure 2. These eigenvectors all share a lack of motion within coordinate numbers 400–500 (residues 133–167) and seem to produce displacements of coordinates in the same regions of the protein, mainly around coordinate numbers 1, 150, 600, and 900 (the N-terminus and residues 50, 200, 300). The eigenvector trajectories were inspected for large concerted atomic motions using interactive graphics. In the first four eigenvectors, similar large rigid body motions of the complete N-terminal and C-terminal domains were observed. This hinge-bending motion appeared to be comparable to the domain displacement observed in the comparison of TLN and NP-cer.[5,6] Figure 3A–D displays the motion along the first four eigenvectors. We have selected the motion along eigenvector 3 for further analysis of the hinge-bending motion, because this motion is approximately periodic, that is, it shows the opening and closing of the active site more than once, and its amplitude is sufficiently large to measure significant differences in interresidue distances. The two structures with the largest difference in total displacement (at 2.6 and 23.2 ps, see below) were extracted from the trajectory along the third eigenvector. For both these structures a C_α–C_α distance matrix was calculated. These matrices were then subtracted, yielding a C_α–C_α distance difference ma-

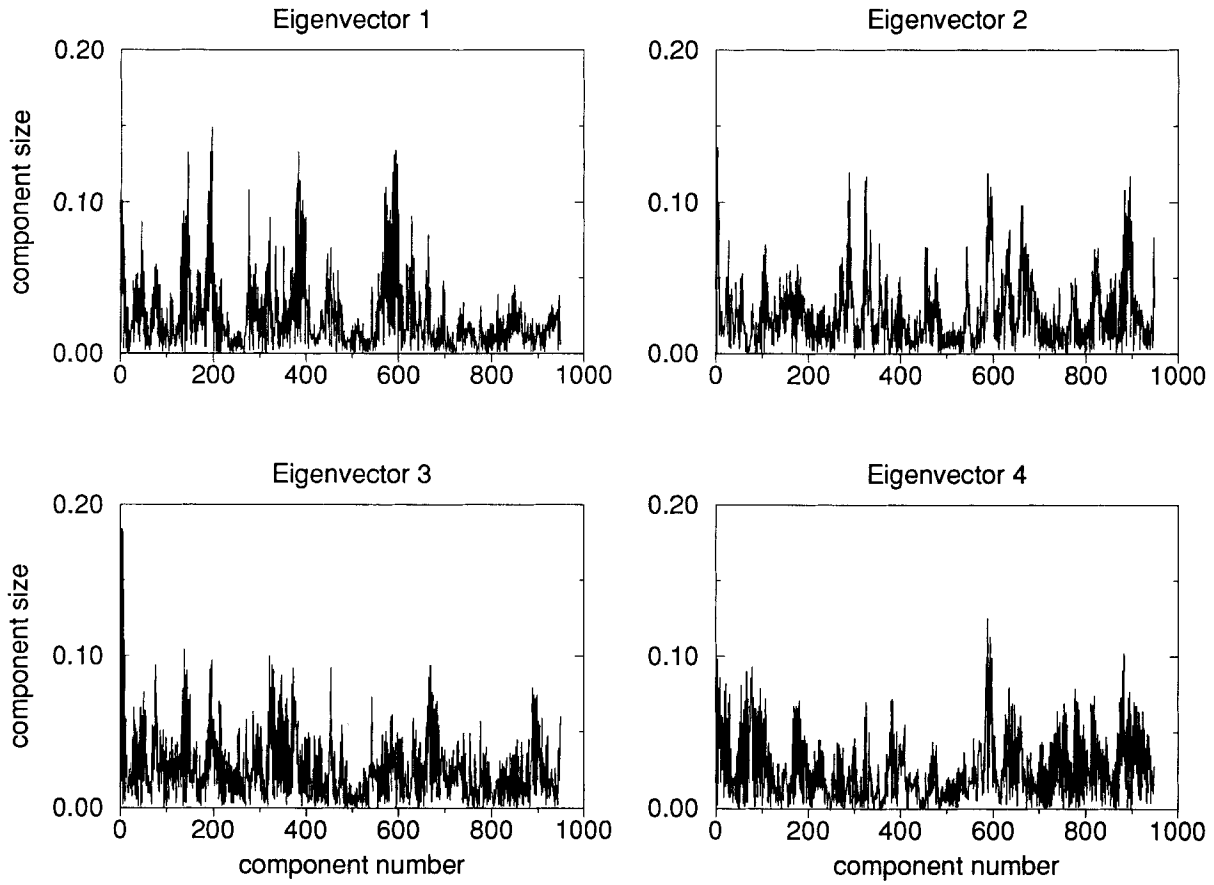

Fig. 2. Components of the first four eigenvectors derived from the solvent simulation (absolute values).

trix,[15] which indicates the differences in all C_α–C_α distances in the two structures. The matrix (Fig. 4) shows that there is a displacement of the N-terminal domain relative to the C-terminal domain, similar to the displacement observed in the comparison of the TLN and NP-cer crystal structures.[5,6] This indicates that the motion described by eigenvector 3 (Figs. 2 and 3) is indeed a hinge-bending motion of the N-terminal and C-terminal domains.

In a previous study essential dynamics analysis of lysozyme MD trajectories revealed large concerted atomic motions.[8] These motions showed relatively large displacements for residues around the active site involved in substrate binding, whereas residues involved in the catalysis were more rigid. Recently, experimental evidence was presented which supports the hypothesis that the large fluctuations of substrate-binding residues observed in the eigenvector motions of lysozyme are important for biological activity.[16] The present analysis of thermolysin shows that there are also large fluctuations around the active site in this enzyme (Figs. 2 and 3). We have analyzed the third eigenvector trajectory to determine the exact position of the hinge-bending residues and to investigate if the catalytic residues in thermolysin are also rigid and surrounded by fluctuating regions. Figure 5 shows the distances between the same residues in two different structures which were superposed either on residues 1–100 or residues 217–316. The plots for the comparison of the NP-cer and TLN crystal structure and the comparison of the 2.6 and 23.2 ps structures from the third eigenvector of the TLN solvent simulation are shown. These plots show that the hinge-bending displacement is similar to the domain displacement observed for the comparison of the TLN and NP-cer structures.[5,6] The plots resulting from the N-terminal and C-terminal superposition intersect several times in the 135–150 region, which suggests that this is a hinge-bending region. This region is the central α-helix in the thermolysin structure which forms the bottom of the active site and which is relatively rigid and at the center of the fluctuation (Figs. 2–5). Glu-143, one of the residues involved in the catalytic cycle, is part of this rigid α-helix, together with two residues that bind the active site zinc (His-142 and His-146).[17] Most residues that are involved in substrate binding (112–115, 203, 157[17]), however, are located in the more mobile domains (Figs. 2–5).

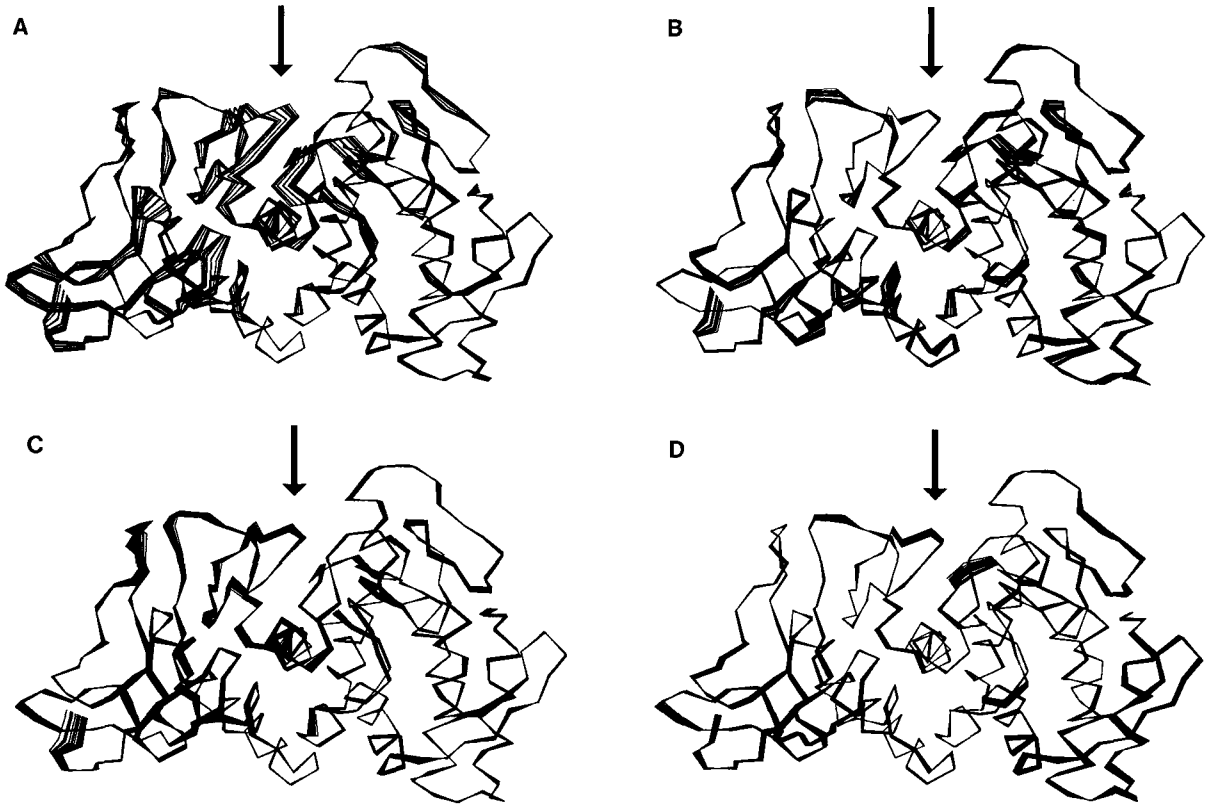

Fig. 3. Representation of the first four eigenvector trajectories constructed by projecting all solvent simulation frames on the first four eigenvectors (**A–D**, respectively) calculated from the solvent simulation covariance matrix. Twenty-five frames are displayed sampled at intervals of 3.6 ps. The arrow indicates the active site cleft with the central α-helix.

Comparison of the Solvent and Vacuum Simulations

We have compared the essential motions of a TLN vacuum simulation (which included crystallographic water molecules) to those in the TLN solvent simulation to investigate the reliability of such a vacuum simulation. Figure 6 shows the eigenvector/eigenvalue plots constructed from the two single (solvent and vacuum) trajectories and the combined trajectory. The plot shows that the eigenvalues of the vacuum and solvent trajectories are similar. However, if these trajectories are concatenated and analyzed by essential dynamics, it appears that the eigenvalue belonging to the first eigenvector is different from the corresponding eigenvalues from the single trajectories. This indicates that there is a difference in the properties of the motions described by the essential eigenvectors coming from the two single trajectories.

By projecting the trajectory frames on a selected eigenvector, the total displacement along that eigenvector and the 3D representation of this displacement can be obtained (an eigenvector trajectory). Figure 7 shows the total displacement along selected eigenvectors from both the vacuum and the

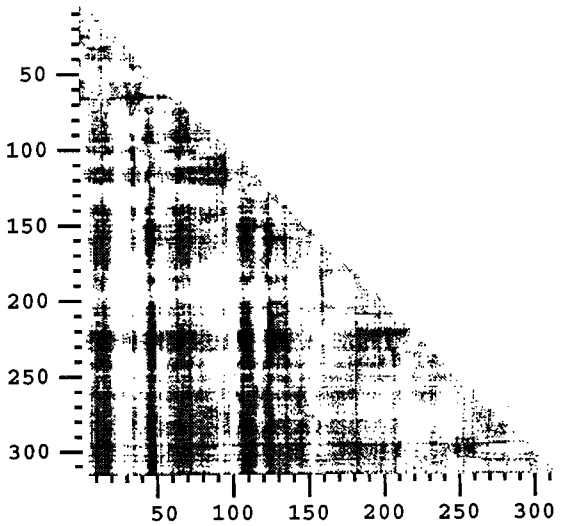

Fig. 4. C_α–C_α distance difference plot[15] constructed by subtracting the C_α–C_α distance matrix of the 23.2 ps structure coming from the third eigenvector motion of the solvent simulation from that of the 2.6 psec structure. The C_α–C_α distance differences are colored using a gray scale. White, difference < 1.0 Å; black, difference > 7.0 Å. A linear gray scale with 7 gray values is used to depict values between these limits.

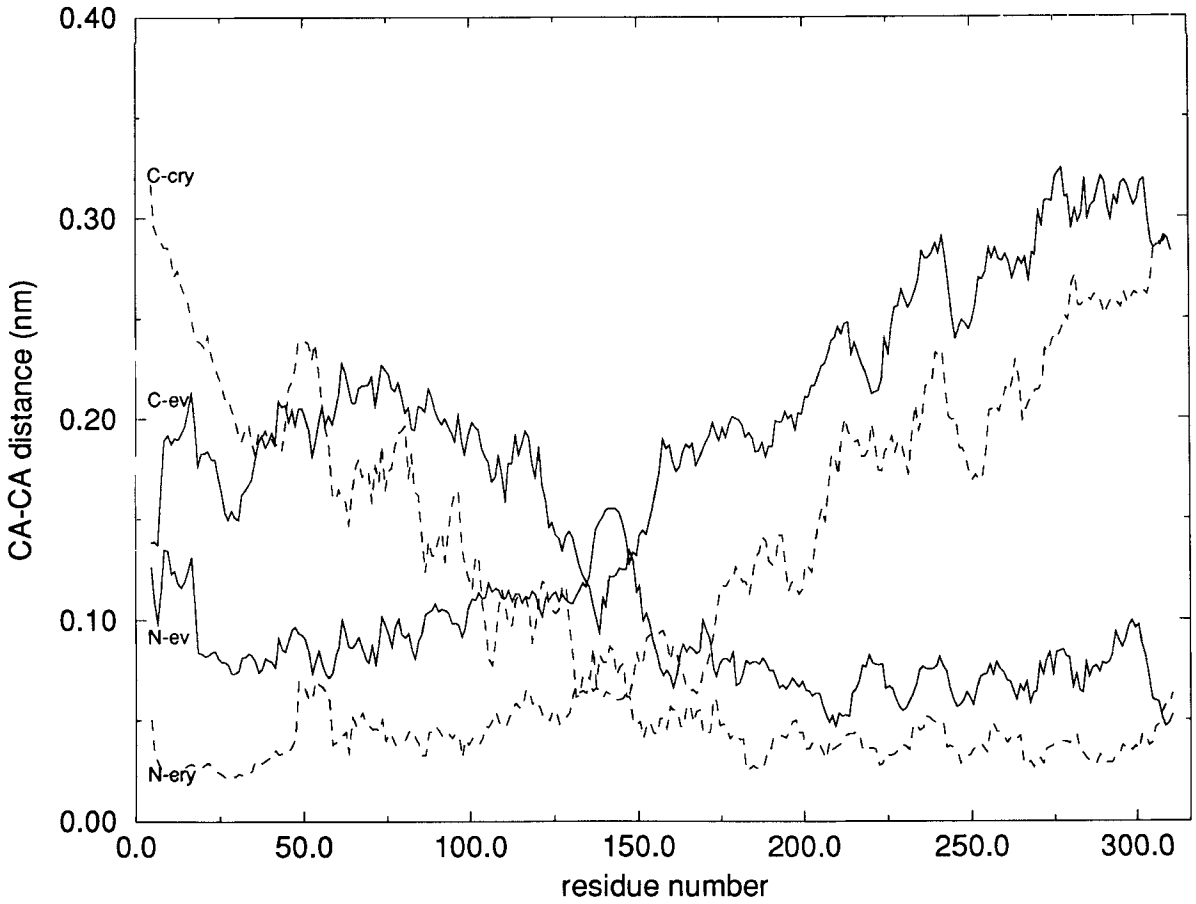

Fig. 5. Difference in C_α–C_α distances for corresponding residues in two superposed structures. The differences in distances are sorted by increasing distance to Thr-26. The solid lines show the differences in distances for the N-terminal and C-terminal superposition of the 2.6 and 23.2 ps solvent simulation structures from the third eigenvector (N-ev and C-ev, respectively). The dashed lines show the differences in distances for the N-terminal and C-terminal superposition of the TLN[2,3] and NP-cer[4,5] crystal structures (N-cry and C-cry, respectively).

solvent simulation. The displacements along the eigenvectors are similar, even for the first eigenvector. The trajectories along the first four eigenvectors from the vacuum simulation revealed hinge-bending motions similar to those observed in the solvent simulation.

The essential space is defined by all eigenvectors which do not have a Gaussian position distribution, that is, are not governed by a harmonic effective potential. To approximately define the essential space, the correlation coefficient between an ideal Gaussian distribution (derived from the eigenvalue of the corresponding eigenvector) and the position distribution of motion along each eigenvector can be plotted against the eigenvector index.[8] This is shown in Figure 8 for the vacuum, solvent, and concatenated trajectories. This figure shows that the first 15 eigenvectors approximately define the essential space, which means that there are only about 15 essential degrees of freedom instead of 948 for all C_α atoms. The correlation coefficient curve (resulting from the comparison between sampled and Gaussian positional distributions, see above) for the combined trajectory is smoother than those of the separate trajectories. This is caused by improvement of the sampling by the use of a longer trajectory, which especially leads to a more accurate definition of the eigenvector motions with Gaussian fluctuations (near constraints).

The projections of the two separate trajectories on the eigenvector set calculated from the combined trajectory were used for further comparisons of the solvent and vacuum trajectories. Figure 9 shows the average projections of the separate trajectories on the eigenvectors calculated from the combined trajectory. Shifts in the average position of the eigenvector motions, and thus the equilibrium structures, can be detected by comparing these curves. There is a large shift in equilibrium structure in the direction described by the first eigenvector calculated from the combined trajectory. Figure 10 shows the positional root mean square fluctuations of the pro-

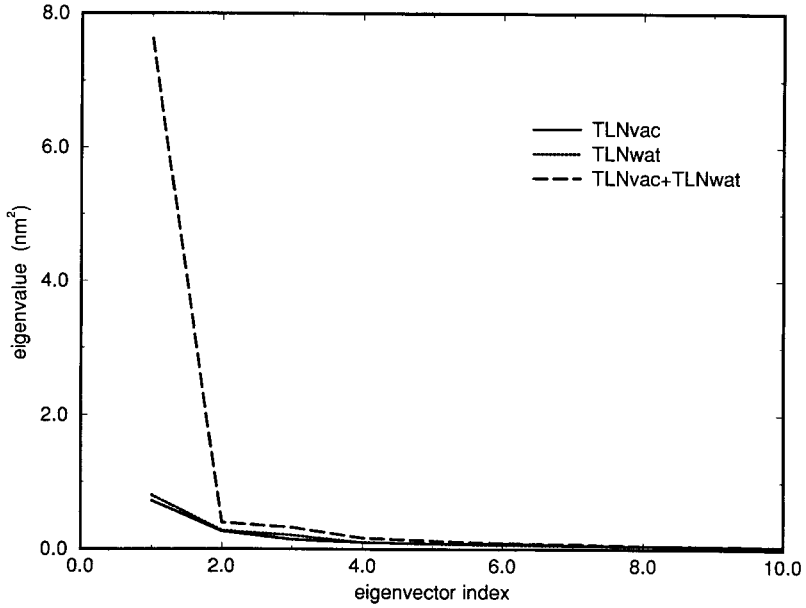

Fig. 6. Eigenvalues derived from the covariance matrices of the solvent (TLNwat), vacuum (TLNvac), and combined (TLNvac + TLNwat) trajectories.

jections of the separate trajectories on the eigenvectors calculated from the combined trajectory. There are differences for the first few eigenvectors. Although there is a large shift in equilibrium structure along the first eigenvector (see Fig. 9), the fluctuations along this direction in the two separate trajectories are similar. There is a significant difference in fluctuation in the directions described by the second and third eigenvectors in the two trajectories. However, the size of the fluctuations indicate that in both trajectories, the directions described by the second and third eigenvector (calculated from the combined trajectory) are part of the essential space.

CONCLUSIONS

Essential Dynamics and Comparison of the Simulations

The essential dynamics analysis of thermolysin has yielded results similar to those from our previous analyses of lysozyme.[8] Although thermolysin is larger than lysozyme (316 against 129 residues), there are also only a few eigenvectors (about 10–15) which construct the essential space (Figs. 1 and 8). The motions along these eigenvectors show large concerted atomic displacements, with a possible biological significance. The comparison of the vacuum and solvent simulations seems to be difficult because of poor statistics, caused by the limited length of the trajectories. The largest difference between the two simulations is described by the first eigenvector calculated from the combined trajectories (see Figs. 9 and 10). There is a large shift in equilibrium structure along this direction, but the fluctuations (in this direction) are similar. In general, however, the essential subspaces of the vacuum and solvent trajectories are similar as is partially demonstrated by the fact that the 3D eigenvector trajectories show similar motions for both simulations.

These conclusions seem to be different from our previous observations concerning the lysozyme vacuum simulation.[8] The motions along the first few eigenvectors of the lysozyme vacuum simulation were significantly different from those of the solvent simulation, indicating that a vacuum simulation does not properly reproduce the solvent simulation essential dynamics properties. However, there is one major difference between the lysozyme vacuum simulation and the thermolysin vacuum simulation. Both crystal structures contain crystallographic water molecules on the surface and in active site clefts.[2,3,18] These water molecules were taken into account in the thermolysin vacuum simulation, but discarded in the lysozyme vacuum simulation. This is a likely cause for the fact that the TLN solvent and vacuum simulations are more similar than those of lysozyme. The essential dynamics properties are influenced by the presence of (internal) water molecules.

Hinge-Bending

The trajectories constructed from the first four eigenvectors show a hinge-bending motion in both simulations, similar to the hinge-bending displacement observed in the comparison of the TLN and NP-cer crystal structures.[5,6] This crystallographic

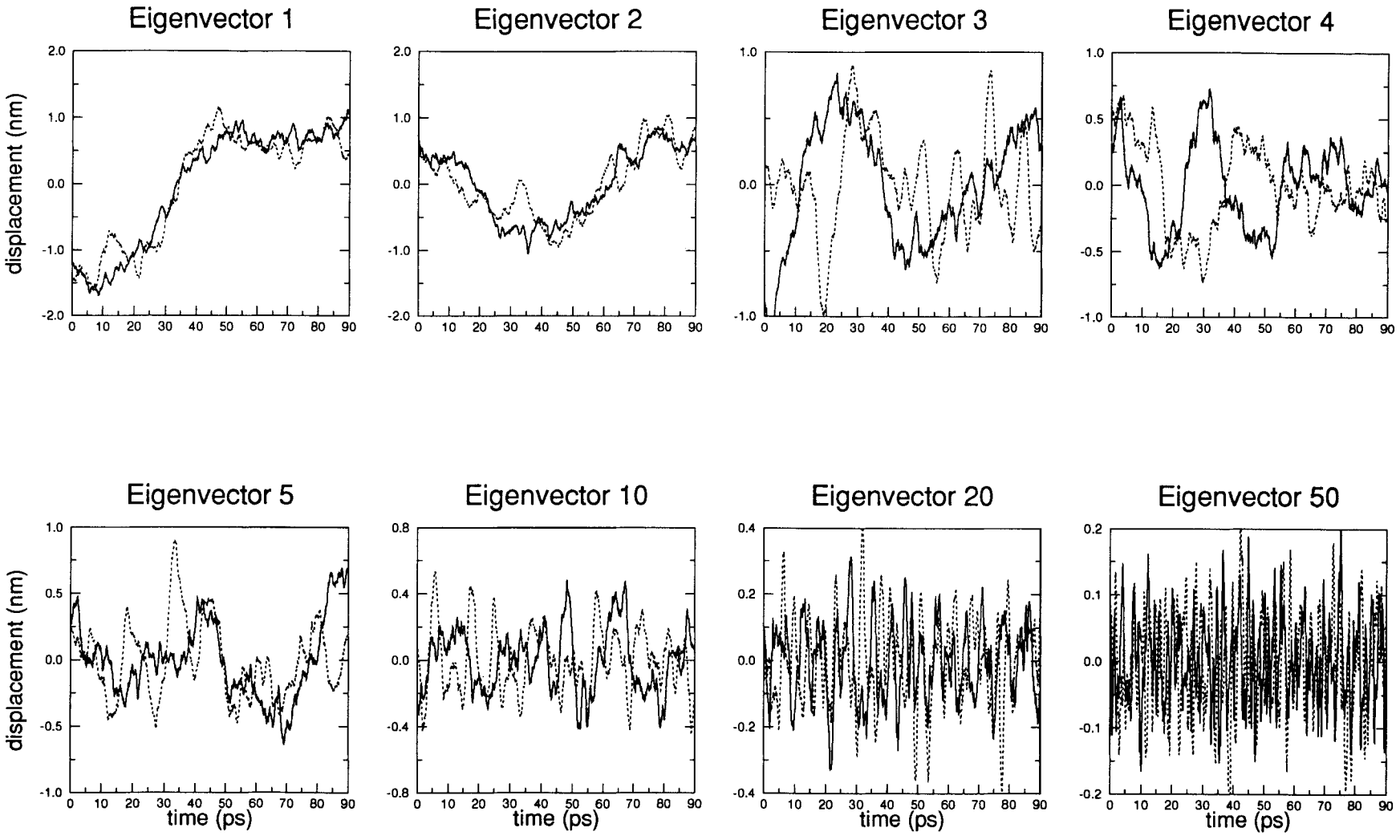

Fig. 7. Projections of the solvent (solid lines) and vacuum (dotted lines) simulation frames on selected eigenvectors.

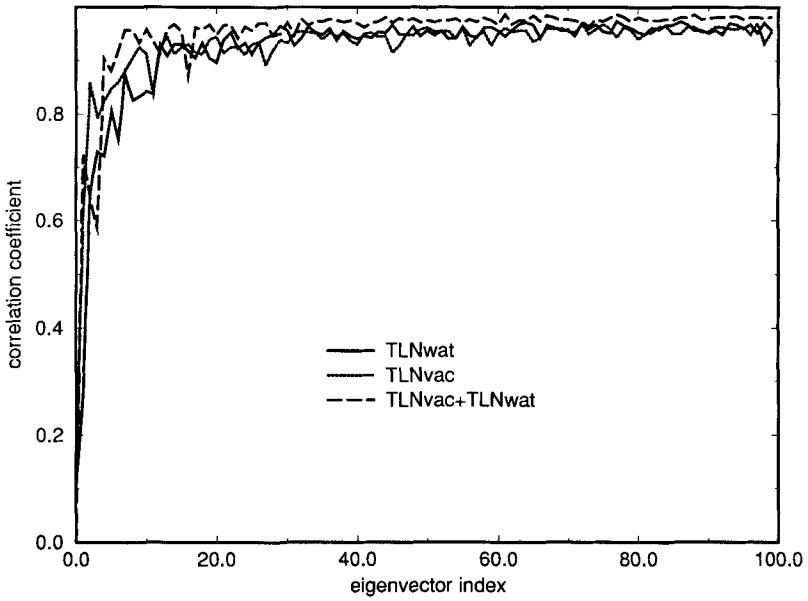

Fig. 8. Correlation coefficients between sampled distributions and ideal Gaussians (derived from the eigenvalue of the corresponding eigenvectors) for the first 100 eigenvectors derived from the vacuum (TLNvac), solvent (TLNwat), and combined (TLNvac + TLNwat) trajectories.

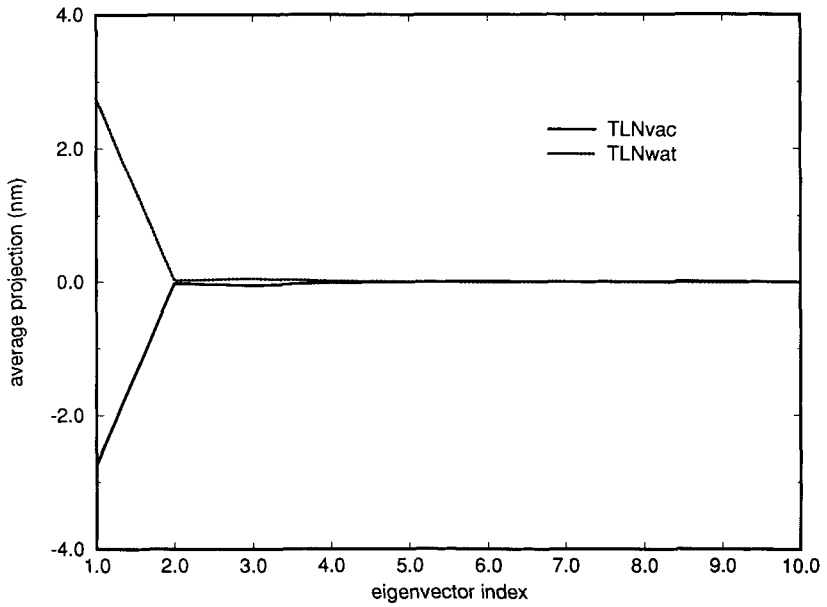

Fig. 9. Average projections of the vacuum (TLNvac) and solvent (TLNwat) trajectories on the eigenvector set derived from the combined trajectory.

comparison led to the hypothesis that residues around position 135 are the hinge-bending residues. On the basis of our analyses of the third eigenvector trajectory, however, we propose a slightly different mechanism. The central α-helix (residues 134–157), containing active site residues, is relatively rigid (in agreement with the crystallographic analysis of TLN,[2,3] which showed relatively low *B*-factors for this region) and there are hinge regions near both ends of this helix (Figs. 2–5). Most residues involved in substrate binding are located in mobile regions. A similar situation was observed for lysozyme.[8] Our analysis, however, cannot show the hinge-bending motion involved in the catalytic cycle of thermolysin

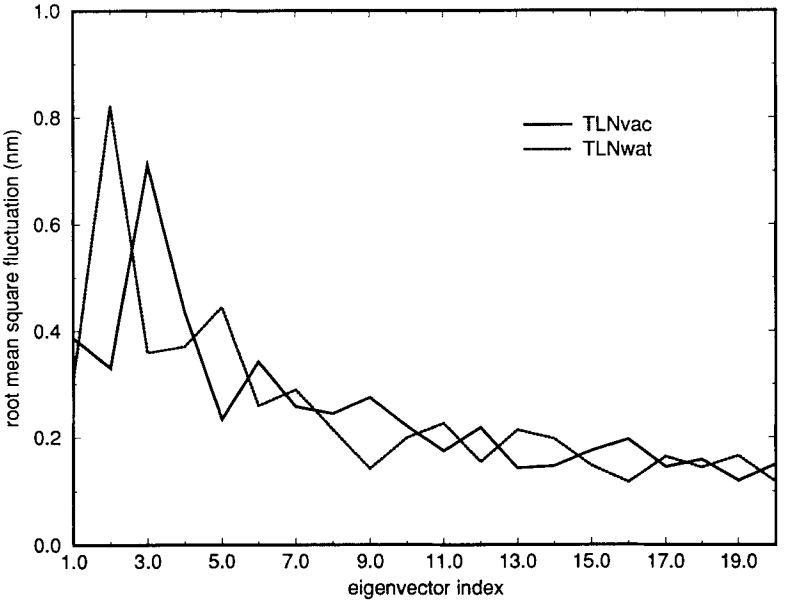

Fig. 10. Root mean square fluctuations in the projections of the vacuum (TLNvac) and solvent (TLNwat) trajectories on the eigenvector set derived from the combined trajectory.

as it takes place in nature. The simulation used was only of limited length (90 ps), whereas motions involved in binding and proteolysis of the substrate take place on a much larger timescale. However, the essential dynamics method identifies the essential degrees of freedom in the mechanical structure of the protein. These degrees of freedom (the essential eigenvectors) largely depend on the interactions between residues and regions in the protein and these interactions are not likely to change much during a longer simulation. It is noteworthy that a 90 ps simulation is long enough to equilibrate the near constraints motions (the Gaussian fluctuations), indicating that the essential space will remain approximately stable on a longer time scale.

REFERENCES

1. Priest, F.G., Atkinson, T., Sherwood, C.R. (eds.) Products and applications. In: "Biotechnology Handbook." New York: Plenum Press, 1989: 293–320.
2. Matthews, B.W., Jansonius, J.N., Colman, P.M., Schoenborn, B.P., Dupourque, D. Three-dimensional structure of thermolysin. Nature (London) 238:37–41, 1972.
3. Holmes, M.A., Matthews, B.W. Structure of thermolysin refined at 1.6 Å resolution. J. Mol. Biol. 160:623–639, 1982.
4. Pauptit, R.A., Karlsson, R., Picot, D., Jenkins, J.A., Niklaus-Reimer, A.-S., Jansonius, J.N. Crystal-structure of neutral protease from *Bacillus-cereus* refined at 3.0 Å resolution and comparison with the homologous but more thermostable enzyme thermolysin. J. Mol. Biol. 199:525–537, 1988.
5. Stark, W., Pauptit, R.A., Wilson, K.S., Jansonius, J.N. The structure of neutral protease from *Bacillus-cereus* at 0.2-nm resolution. Eur. J. Biochem. 207:781–791, 1992.
6. Holland, D.R., Tronrud, D.E., Pley, H.W., Flaherty, K.M., Stark, W., Jansonius, J.N., McKay, D.B., Matthews, B.W. Structural comparison suggests that thermolysin and related neutral proteases undergo hinge-bending motion during catalysis. Biochemistry 31:11310–11316, 1992.
7. VanAalten, D.M.F., Vriend, G., Linssen, A.B.M., Venema, G., Berendsen, H.J.C., Eijsink, V.G.H. Thermal stability of thermolysin-like proteases: long range effects of a critical mutation revealed by molecular dynamics simulations. Protein Eng., submitted.
8. Amadei, A., Linssen, A.B.M., Berendsen, H.J.C. Essential dynamics of proteins. Proteins 17:412–425, 1993.
9. Van Gunsteren, W.F., Berendsen, H.J.C., BIOMOS, Biomolecular Software, Laboratory of Physical Chemistry, University of Groningen, The Netherlands, 1987.
10. Berendsen, H.J.C., Grigera, J.R., Straatsma, T.P. The missing term in effective pair potentials. J. Phys. Chem. 91:6269–6271, 1987.
11. Brooks, B., Karplus, M. Harmonic dynamics of proteins—normal-modes and fluctuations in bovine pancreatic trypsin-inhibitor. Proc. Natl. Acad. Sci. U.S.A. 80:6571–6575, 1983.
12. Levitt, M., Sander, C. Stern, P.S. Protein normal-mode dynamics: Trypsin inhibitor, crambin, ribonuclease and lysozyme. J. Mol. Biol. 181:423–447, 1985.
13. Vriend, G. WHAT IF—A molecular modeling and drug design program. J. Mol. Graph. 8:52–56, 1990.
14. Scheek, R.M., VanNuland, N.A.J, DeGroot, B.L., Linssen, A.B.M., Amadei, A. Structure from NMR and molecular dynamics: Distance restraining inhibits motion in the essential subspace. Manuscript in preparation.
15. Nishikawa, K., Ooi, T., Isogai, Y., Saito, N. Tertiary structure of proteins. I. Representation and computation of the conformations. J. Phys. Soc. (Jpn) 32:1331–1337, 1972.
16. Imoto, T., Ueda, T., Tamura, T., Isakari, Y., Abe, Y., Inoue, M., Miki, T., Kawano, K., Yamada, H. Lysozyme requires fluctuation of the active site for the manifestation of activity. Protein Eng. 7:743–748, 1994.
17. Kester, W.R., Matthews, B.W. Crystallographic study of the binding of dipeptide inhibitors to thermolysin: Implications for the mechanism of catalysis. Biochemistry 16: 2506–2516, 1977.
18. Blake, C.C.F., Koenig, D.F., Mair, G.A., North, A.C.T., Philips, D.C., Sarma, V.R. Structure of hen egg-white lysozyme. Nature (London) 206:757–761, 1965.